


Lanthanide-Doped Upconversion Nanomaterials: Recent Advances and Applications

Dongkyu Kang^{1,2,†}, Eunyoung Jeon^{1,†}, Suyeon Kim¹ & Joonseok Lee^{1,*} 

Received: 8 January, 2020 / Accepted: 4 February, 2020 / Published online: 16 March, 2020
©The Korean BioChip Society and Springer 2020

Abstract Lanthanide-doped upconversion nanomaterials are well known for converting near-infrared (NIR) excitation photons into visible, ultraviolet, and NIR emission photons. Excitation of NIR light offers low autofluorescence background and high penetration depth in biological environments due to the reduced light scattering. Consequently, these have attracted considerable interest because their exceptional optical properties have led to applications in diverse areas such as bioassays, biomedical imaging, and forensics; these properties are, namely: large anti-Stokes shifts, sharp emission spectra and long excited-state lifetimes. The nanomaterials can be utilized for a variety of applications including detection of various analytes, bioimaging, therapies, energy conversion, and security. In this review, we briefly describe the upconversion luminescence process, effective synthetic approaches, and recent literature that elucidate the exceptional properties of these materials and its applications.

Keywords: Nanoparticles, Lanthanides, Upconversion, Anti-Stokes, Luminescence, Energy transfer

Introduction

Luminescent signal-based applications continue to attract significant attention because of their potential in fields of biosensing, biomedical imaging, therapies, energy conversion, and also security. In the early days of luminescent materials, organic dyes and quantum dots (QDs) were reported for use in numerous applications^{1–5}. Organic dyes have a good biocompatibility, relatively high fluorescence intensity and facilitate the easy modification of the surface for covalent conjugations. However, photobleaching, chemical degradation, and broad emission spectra with long tailing limit their practical applications⁶. Due to the rapid development of nanotechnology, QDs have emerged as an alternative fluorescent material that possesses the unique properties of an intense and size-tunable emission, a good photostability, an excitation in the ultraviolet (UV) region, and narrow emission bands. These QDs have led to the various applications in fluorescence resonance energy transfer (FRET) based analysis, tissue imaging, and electrochemical energy conversion. Unfortunately, due to the inherent cytotoxicity of heavy metal-based QDs, their applications have been limited⁷. Moreover, QDs typically require UV radiation, which is potentially harmful to living cells and biomolecules, including proteins and nucleic acids.

In contrast to QDs, lanthanide-doped upconversion nanoparticles (UCNPs) can convert near-infrared (NIR) light into UV, visible, or NIR light through a nonlinear optical phenomenon that is known as anti-Stokes emission, wherein two or more low-energy photons are absorbed leading to a high-energy emission. Different from traditional fluorescent materials,

¹Molecular Recognition Research Center, Korea Institute of Science and Technology (KIST), Division of Nano and Information Technology, KIST School, Korea University of Science and Technology (UST), 5, Hwarang-ro 14-gil, Seongbuk-gu, Seoul 02792, Republic of Korea

²Departments of Material Science and Engineering, Yonsei University, 50, Yonsei-ro, Seodaemun-gu, Seoul 03722, Republic of Korea

[†]These authors contributed equally.

*Correspondence and requests for materials should be addressed to J.S. Lee (✉ jslee@kist.re.kr)

UCNPs possess the following powerful advantages: 1) an outstanding signal-to-noise ratio offers improved detection sensitivity, owing to less autofluorescence in NIR diagnostic window range of 700 – 1100 nm. 2) Further, the utilization of the NIR excitation light allows for deeper light penetration and reduced photo-damage effects, and 3) the lack of toxicity enables long-term use in biological environments. Additional advantages of UCNPs are, namely: narrow emission peaks, large anti-Stokes shifts, and good chemical- as well as photo-stability⁸. Over the past decade, these unique properties of UCNPs have led to successful applications, including background-free biological sensing, high contrast biomedical imaging, energy conversion, and security⁹. Moreover, UCNPs with various dopants (e.g., Gd, Sm, etc) can combine luminescent imaging with other imaging modalities that pave the way for novel theranostic applications such as magnetic resonance imaging (MRI) as well as computed tomography (CT)¹⁰. In this review, we focus on the recent advances in design and applications of UCNPs. We categorized our review to cover up-conversion luminescence mechanism, synthesis methods, and the luminescence signal-based analysis of target markers. Moreover, it elucidates the diagnosis and therapeutic applications. Solar light-induced energy conversion applications have also been addressed along with luminescence signal-based applications for security (See Figure 1).

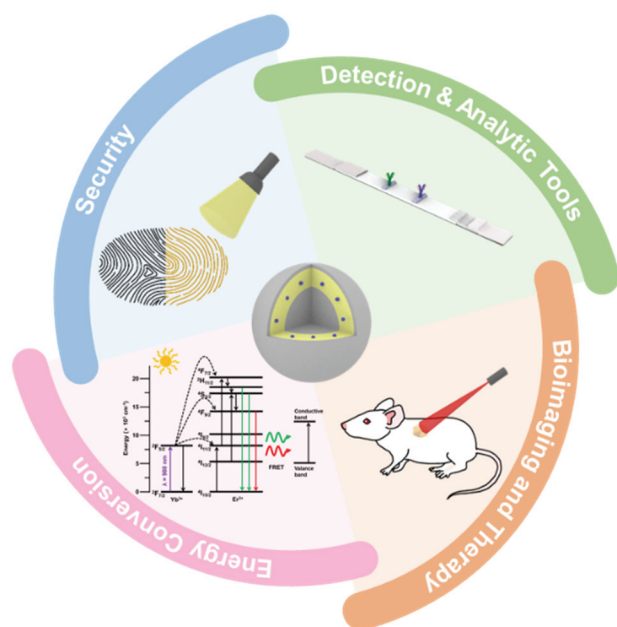


Figure 1. Schematic illustration of upconversion nanomaterial applications in diverse fields.

Upconversion Luminescence Mechanism

Upconversion is a nonlinear optical process of converting low energy (e.g., NIR light) electronic transitions into higher energy electronic transitions (e.g., visible or UV light) and can, therefore, be ascribed as an anti-Stokes mechanism. Upconversion luminescence (UCL) emissions are generated by optical transitions within the partially filled $4f$ orbitals of lanthanide ions¹¹. The theoretical possibility of this phenomenon in ion-doped solid-state infrared quantum counters was first introduced by Nicolaas Bloembergen in 1959¹². The mechanism of upconversion process has been extensively studied in recent years and can be divided into five main classes, which include excited state absorption, energy transfer upconversion (ETU), photon avalanche, cooperative sensitization upconversion, and energy migration upconversion. It should be noted that among these five proposed mechanisms the ETU mechanism of energy transfer strongly dominates¹³. Thus, we will focus on the description of the ETU process here.

Energy Transfer Upconversion

The ETU process takes place between the sensitizer and activator system with a non-radiative energy transfer pathway that exists between two neighboring ions as illustrated in Figure 2A. In a typical ETU process, the photon excites an ion known as the sensitizer from the ground state (G) to enter a long-lived intermediate, metastable excited state of the sensitizer ion and energy transfer then occurs from the sensitizer ion to the metastable level 1 state (E1) of the activator ion. Continuously, the photon then promotes this ion from the activator E1 state to the higher, metastable excited state 2 (E2). When the sensitizer ion relaxes back to G state, the activators populated in the E2 state radiatively relax to the G state and emit upconversion photons. The efficiency of the ETU process depends on the distance between the sensitizers and activators, which relies on the concentrations of dopant ions. As a result, doping is the most widely implemented strategy in the design of upconversion nanomaterials.

Selection of Host Materials, Sensitizers and Activators for Tunable Emission

Upconversion nanomaterials are mainly composed of a host matrix, a sensitizer ion and an activator ion. Appropriate selection of host materials is essential for an efficient upconversion process. Recently, the upconversion process has been reported in numerous

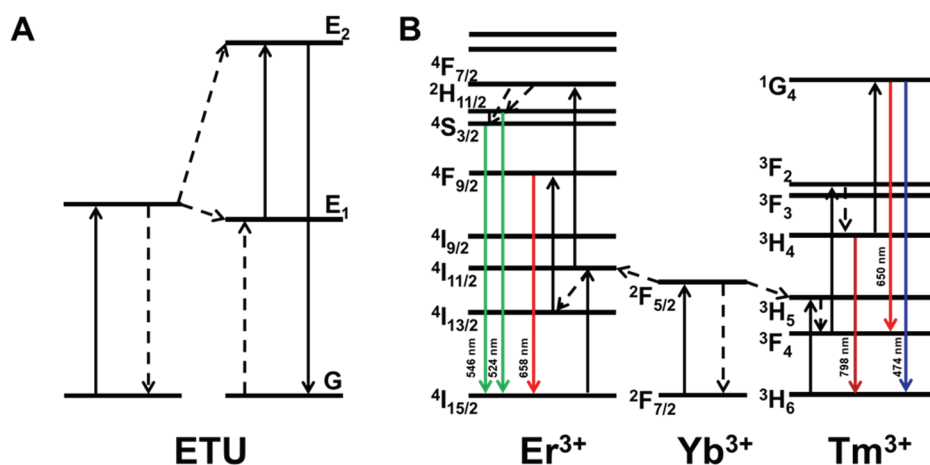


Figure 2. Schematic illustration of energy transfer process for (A) ETU and (B) Energy transfer mechanism of NaYF₄:Yb,Er/Tm co-doped upconversion nanomaterials under 980 nm excitation.

nanoscale host matrixes such as fluorides, oxides, phosphates, and vanadates¹⁴⁻¹⁷. Among these types of host materials, fluorides have been shown to be a superior host material for the upconversion process, since fluorides show low phonon energies and high chemical stability¹⁸. Thus, NaYF₄ has become the most popular host material for high-quality UCNPs.

The most commonly used lanthanide dopant ion combinations for the fabrication of upconversion nanomaterials are Yb³⁺/Er³⁺ and Yb³⁺/Tm³⁺. Note that other ions with partially filled 4*f* orbitals can also be used as dopants ion. As shown in Figure 2B, Yb³⁺ is employed as the sensitizer for Tm³⁺ or Er³⁺. Co-doped Yb³⁺ systems have a large absorption cross-section in the NIR region at 980 nm. NIR photons are firstly absorbed by the Yb³⁺ ion sensitizer and then are transferred to a near activator emitting center (*e.g.*, Er³⁺ and Tm³⁺) via the ETU process. Radiative relaxation of the excited activator ions emits photons each red, green, and blue emissions (Figure 2)^{19,20}. The emission intensity of upconversion nanomaterials can be affected by numerous factors, such as dopants concentrations, particle size, morphology, host material, crystalline phase and method of preparation²¹⁻²³. Upconverting processes of multiple-step between lanthanide ions commonly have a relatively low conversion quantum yield. Therefore, the enhancement of the upconversion intensity can be achieved by annealing treatment or shell formation for surface passivation which minimizes luminescence quenching.

Synthesis of Upconversion Nanomaterials

To obtain high-quality upconversion nanomaterials, many efforts have been devoted to the exploration of

developing facile synthetic methods such as co-precipitation and thermal decomposition. One of the main goals in the many synthetic methods is the reproducibility of monodispersed upconversion nanomaterial. These particles should exhibit a narrow size distribution, be phase-pure, and be highly soluble in aqueous solutions for biological applications. In the following section, we discuss the common synthetic methods of co-precipitation and thermal decomposition. Synthetic process of upconversion nanomaterials is briefly described in Figure 3.

Thermal Decomposition Method

In a typical thermal decomposition procedure for fluoride-based nanomaterials, a rare earth metal trifluoroacetate (RE(CF₃COO)₃) is thermally decomposed to provide the corresponding metal and fluoride ions. Novel synthesis of pure-phase and monodisperse LaF₃ triangular nanoplates from a single-source precursor of RE(CF₃COO)₃ was first reported by the Zhang et al. through the thermal decomposition²⁴. This method was further applied to alkali lanthanide tetrafluoride-based UCNPs (NaREF₄). Mai et al. reported a general synthetic strategy for crystalline, monodisperse NaREF₄ UCNPs via metal/RE-trifluoroacetate precursors (Na(CF₃COO) and RE(CF₃COO)₃)²⁵. The solvent for this procedure consists of a coordinating solvent and a non-coordinating solvent. To provide a high-temperature environment, 1-octadecene (ODE) was used as the non-coordinating solvent (b.p.315 °C), and the reaction was performed under a protective layer of argon gas. As coordinating solvents, oleic acid (OA) and oleyamine (OM) were used to prevent aggregation by capping the surface of

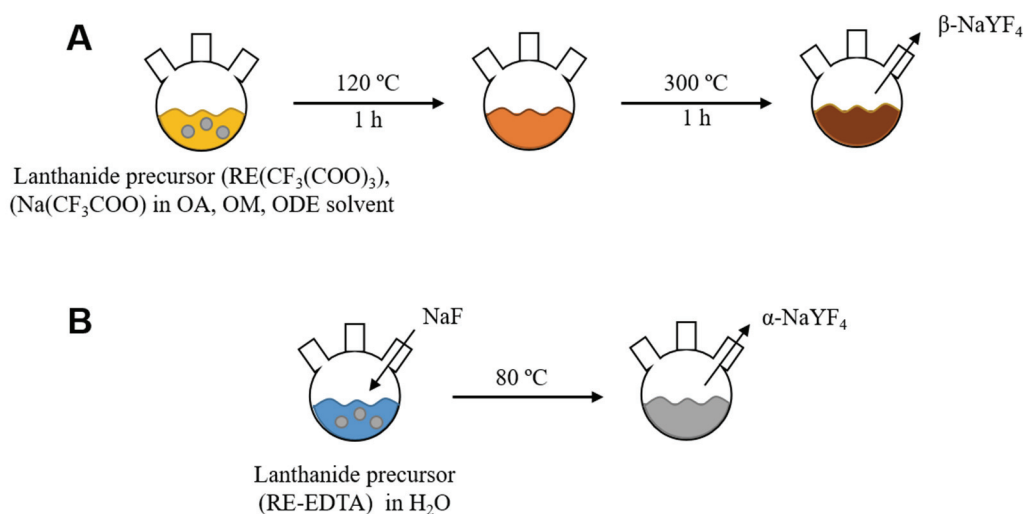


Figure 3. Synthesis methods of upconversion nanomaterials. (A) Thermal decomposition method (B) Co-precipitation method.

nanoparticles. Using a single solvent trioctylphosphine oxide (TOPO) Shan et al. reported a new thermal decomposition method such that the energy barrier of the cubic to hexagonal phase transition was considerably reduced by using TOPO as the solvent, providing a more efficient way to form hexagonal phase UCNPs a rather than OA/OM/ODE combined solvent system²⁶.

Co-Precipitation Method

Co-precipitation method is the easiest way for synthesizing lanthanide-doped upconversion nanomaterials. Yi et al. first reported the co-precipitation method for synthesizing $\text{NaYF}_4:\text{Yb},\text{Er}$ with the aid of ethylenediamine tetraacetic acid (EDTA)²⁷. The cubic-phase of $\alpha\text{-NaYF}_4:\text{Yb},\text{Er}$ resulted from that co-precipitation procedure via a rare earth (RE) complex of EDTA with a NaF solution. To increase the UCL emission intensity, an annealing treatment was applied that resulted in the phase transition from a cubic to hexagonal phase. This transition is critical, because of the weak luminescence emission intensity of the cubic-phase upconversion nanomaterials ($\alpha\text{-NaYF}_4$). However, aggregation of UCNPs after the annealing process limits their potential applications. Moreover, the capping ligands EDTA could be carbonized after the annealing process, reducing the hydrophilicity of the upconversion nanomaterials. Therefore, further surface modifications are required to improve the water-solubility of upconversion nanomaterials. For example, polyethylenimine (PEI), an organic polymer surfactant, is used as a surface ligand to improve water-solubility and prevent particle aggregation.

Exploiting Applications of Upconversion Nanomaterials

Detection and Analytical Platform

Upconversion nanomaterial signal-based detection assays have the powerful property of low signal-to-noise levels in the NIR-region, leading to an outstanding limit of detection (LOD) in biological environments. Therefore, these materials have been utilized in sensitive and specific methods for the detection of biomolecules, pH changes, metal ions and temperature. The assay methods are categorized as heterogeneous assays and homogeneous assays. Heterogeneous assays are commonly carried out in a solid-phase system that requires several wash steps or sample preparation steps, while a homogeneous assay is generally performed in a liquid-phase, where an optical measurement utilizes a simple mix and read-out system.

Heterogeneous Assay

To detect target analytes, the heterogeneous assay method utilizes highly specific recognition with binding affinity between the target analytes and functionalized UCNPs, immobilized on a solid-phase substrate. Based on the upconversion nanomaterials, heterogeneous assays have been successfully explored and exhibited improved LOD²⁸⁻³¹. One of the most promising assays platforms, the lateral flow assay (LFA) platform has advantages, providing point-of-care and on-site monitoring extensively established for the detection of various analytes. As shown in

Figure 4A, an avian influenza virus (AIV) assay has a LOD 10-times lower than that of the commercial gold nanoparticle-based AIV LFA kit, even with opaque samples³². The LOD of the AIV LFA kit for low pathogenicity avian influenza (LPAI) H5N2 and high pathogenicity avian influenza (HPAI) H5N6 viruses was 10^2 and $10^{3.5}$ EID₅₀/mL, respectively³². Recently, a microplate assay based on UCL has been developed to detect trace amounts of analytes in fluid samples. For example, an assay for the biomolecule

alpha-fetoprotein, a biomarker of liver cancer, has been developed with a dynamic working range of 0.01–40 ng/mL and a LOD of 5.3 pg/mL³³. The UCNP signal is based on enzyme-linked immunosorbent assays (ELISA). This method can be employed for other analytes that are commonly detected by conventional ELISA. For example, the micropollutant diclofenac was detected in solution with LOD of 0.05 ng/mL, using ELISA type based UCNPs signals³⁴.

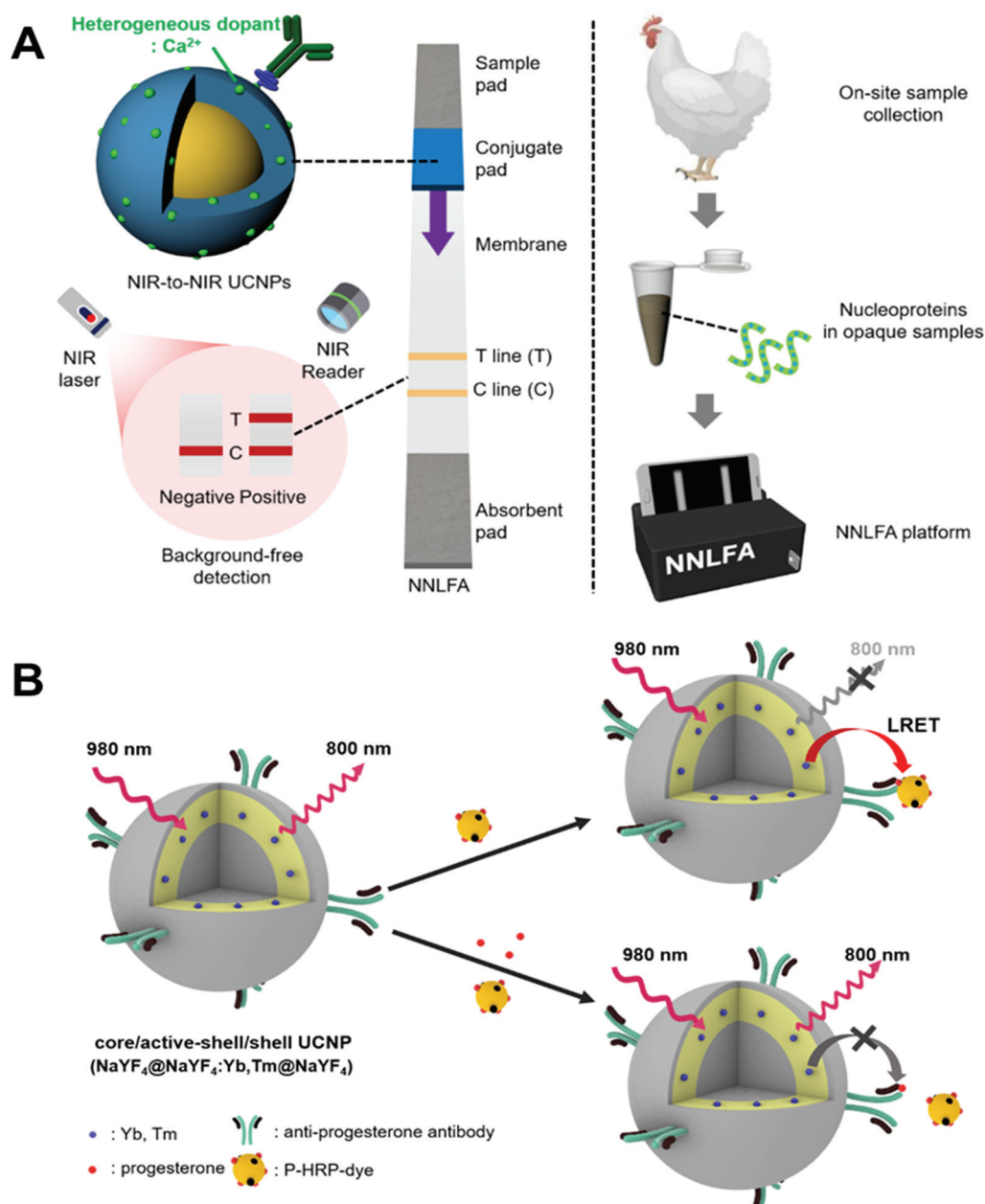


Figure 4. Upconversion nanomaterial based heterogeneous and homogeneous assay (A) Lateral flow immunoassay for detection of AIV³², (B) Competitive immunoassay for detection of progesterone³⁸. Images reproduced from the references with permission.

Homogeneous Assay

In contrast to heterogeneous methods that may require laborious separation or washing steps, homogeneous assays do not require substrate immobilization or washing steps and are performed by a simple mix and readout procedure directly performed in the liquid phase. The homogeneous assay is commonly based on the distance-dependent energy transfer (*e.g.*, FRET or LRET) between the energy donor and the energy acceptor³⁵. To achieve a sensitive assay with a low LOD, the factors to be considered for efficient energy transfer are the distance between the donors and acceptors and spectral overlap between the emission of the donor and the absorption of acceptors. In a typical LRET-based homogeneous assay, upconversion nanomaterials are first excited by NIR irradiation and then non-radiative energy transfer occurs to the spectrally overlapping acceptors, leading to the luminescence quenching of UCL emission signal. The LRET-based homogeneous assays have greatly improved LOD and use a simple readout process^{36,37}. As shown in Figure 4B, progesterone was detected by the sensor platform based on a NIR-to-NIR signal LRET system via competitive immunoassay. The LOD was calculated to be 1.40 pg/mL, which is 35 times lower than that of commercial progesterone ELISA kit³⁸. The LRET-based homogeneous assay has further been used for the detection of heavy metals Hg²⁺ and Pb²⁺ in aqueous solutions and to successfully detect pH changes³⁹⁻⁴².

Diagnosis and Treatment

Biomedical Imaging

Upconversion nanomaterials play a critical role in biomedical techniques, such as monitoring and treatment as well as MRI and CT imaging due to the upconversion process where NIR photons are converted into higher energy photons like visible emission. Upconversion nanomaterials have the advantages of low toxicity, deep light penetration and low autofluorescence. Lanthanide-doped (Gd³⁺/Yb³⁺/Nd³⁺/Er³⁺) UCNPs can be used as multifunctional contrast agents with magnetic, optical and x-ray properties⁴³. Yb³⁺-doped UCNPs have been widely explored but applications are limited due to rising of local temperatures and overheating, which could induce undesired death or injury to a normal cell. To resolve these limits, Nd³⁺ has been employed as a photosensitizer (PS) for reducing the overheating, and to adjust the excitation wavelength at 980 nm to a more biocompatible wave-

length of 808 nm (Figure 5A)^{44,45}. In recent research, Gd³⁺ has been used in UCNPs to enhance the T₁-weighted MRI signal and Dy³⁺ has been used as a contrast agent for T₂-weighted MRI and enhancing CT imaging due to high k-edge values (Figure 5B)^{43,46}. Further, Sun et al. reported in vivo multimodal imaging (UCL, MRI, CT) using NaGdF₄:Yb,Er UCNPs and it showed strong contrast at the tumor site⁴⁶. By synthesizing appropriate lanthanide-doped UCNPs, multimodal imaging can offer highly accurate information and image-guided therapy⁴⁴.

Therapeutics

The non-invasive phototherapy is mainly divided into photodynamic therapy (PDT) and photothermal therapy (PTT). PDT can produce reactive-oxygen species (ROS) by activating the PS⁴⁷. The penetration ability of UV-visible light is limited, but NIR light has a deeper-penetrable ability. So, the UCNPs absorb NIR light and emit UV-visible light, which can activate the PSs to produce cytotoxic ROS⁴⁸. The generation of ROS can cause cancer cell apoptosis or necrosis^{46,47}. Also, ROS have been implicated in Alzheimer's disease. For example, Lee et al. reported that NaYF₄:Yb,Er UCNPs emit visible light under the NIR irradiation and photoexcited rose Bengal (RB) as a PS generates ROS, which can suppress the aggregation of β -amyloid (A β)⁴⁸.

In PTT, NIR light is converted into localized heat energy, inducing cellular hyperthermia⁴⁶. PTT relies on photothermal agents to generate heat and increase temperature upon NIR light irradiation⁴⁹. Various NPs, such as carbon nanomaterials, transition metal sulfides and oxides, have been proposed as photothermal agents. In particular, plasmonic nanomaterials can be easily used in PTT due to the localized surface plasmon resonance. For example, Sun et al. reported that gold nanorod (NR) dimers serve as strong PTT agents and the UCNPs serve as a PDT agent. The tumor treatment with only PTT or PDT is not enough to induce cell death completely. However, the combination of PTT and PDT can provide superior effects like sufficient or complete tumor elimination⁴⁶.

Solar-to-Chemical Energy Conversion

Water Splitting

In terms of energy, sunlight reaching the Earth's surface is approximately 53% IR (above 700 nm), 42% visible (400 to 700 nm), and 3% UV (below 400 nm)⁵⁰.

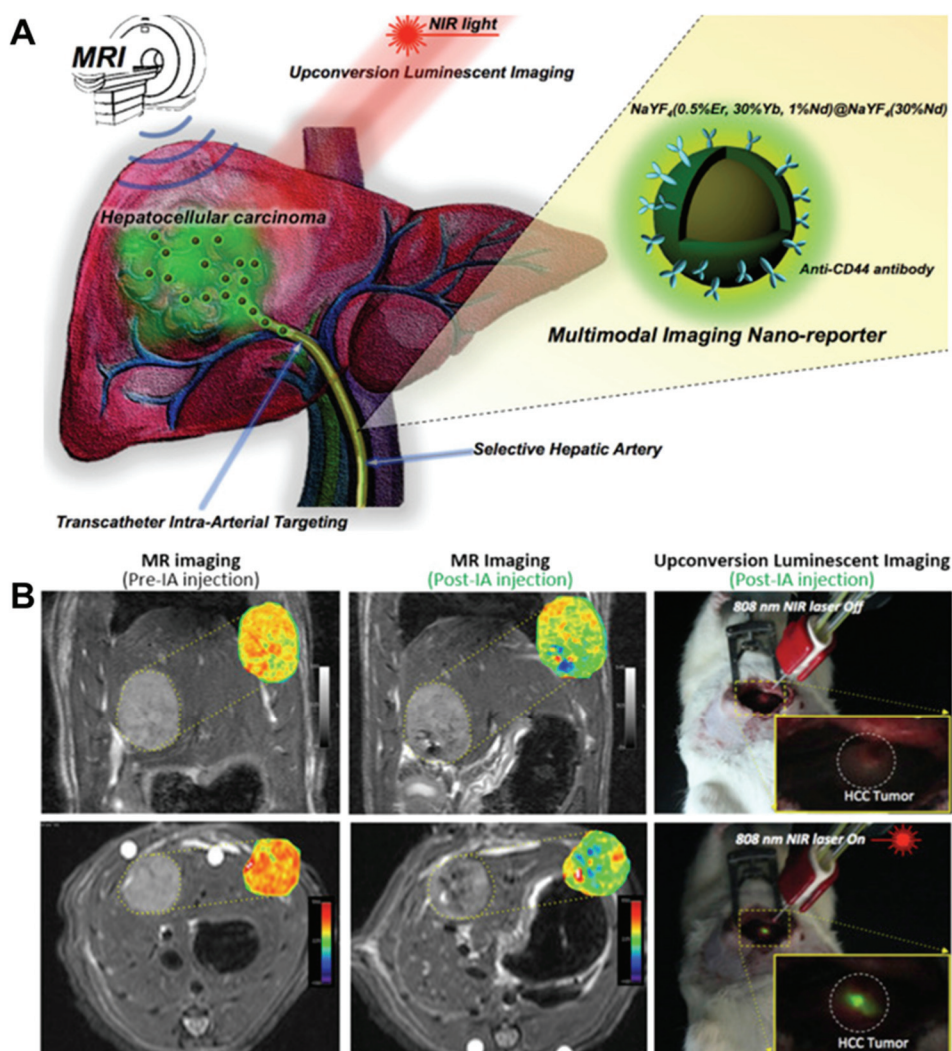


Figure 5. (A) Schematic of multimodal MR/Upconversion luminescent imaging of hepatocellular carcinoma (HCC) tumor using transcatheter hepatic intra-arterial (IA) targeted UCNPs⁴⁴, (B) T₂-weighted MR images acquired before and after UCNP injection and T₂ maps (insets) of HCC tumor regions; (right) intraoperative upconversion luminescent imaging⁴⁴. Images reproduced from the references with permission.

Solar-to-chemical energy conversion is one of the ultimate goals for researchers because it can allow sustainable production and the carbon-neutral use of chemicals⁵¹. Therefore, photon upconversion of infrared light is a promising approach to efficient light harvesting. Kim and co-workers fabricated a photoelectrochemical water splitting device using a versatile layer-by-layer (LbL) assembly method⁵². UCNPs, Ag nanoparticles, and polyoxometalate catalysts have been used for NIR light emission, plasmonic effects, and water oxidation catalytic activity, respectively (Figure 6A). Figure 6B shows that the upconversion emission was significantly improved after the deposition of LbL-assembled hybrid films, which synergis-

tically enhanced the performance of water oxidation devices. The photocurrent density at 1.23 V versus reversible hydrogen electrode under 980 nm NIR light irradiation was improved by about five fold after the LbL deposition.

Cofactor Regeneration

Green plants use nicotinamide cofactors [NAD(P)H], redox chemicals carrying electrons, as a reducing power for conversion of carbon dioxide to carbohydrates in the Calvin cycle⁵¹. Therefore, nanobiocatalysis-based artificial photosynthesis aims to reassemble man-made PSs, electron mediators, electron donors,

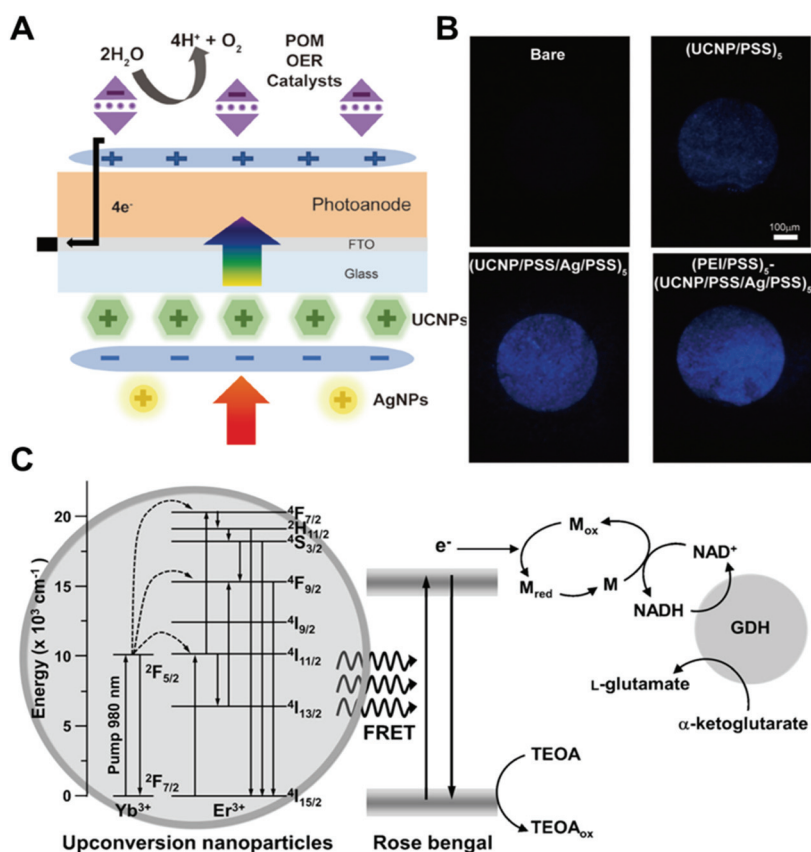


Figure 6. Solar-to-chemical energy conversion by upconversion luminescence process. (A) Upconversion nanoparticle-based photoelectrochemical water splitting device⁵², (B) Photographs of upconversion nanoparticle complex⁵², (C) Cofactor regeneration under NIR illumination⁵⁴. Images reproduced from the references with permission.

and redox enzymes for photochemical synthesis of valuable chemicals through cofactor regeneration process⁵³. Figure 5C shows NIR-light-driven biocatalytic artificial photosynthesis using efficient photon-conversion through FRET with silica-coated UCNP as donor and RB as acceptor⁵⁴. NIR-excited electrons are transferred to an electron mediator (i.e., a rhodium(III) catalyst) through FRET and reduced NAD^+ to NADH, resulting in the synthesis of l-glutamate by cofactor-dependent l-glutamate dehydrogenase. The photoenzymatic conversion of substrate to product is facilitated with upconversion complexes through NIR light-driven photochemical cofactor regeneration. The results show that UCNP are promising light harvesters for NIR light-to-chemical conversion processes.

Security Printing

Anti-Counterfeiting

UCL-based ink is promising as an anti-counterfeiting application, since UCL ink is invisible under ambient

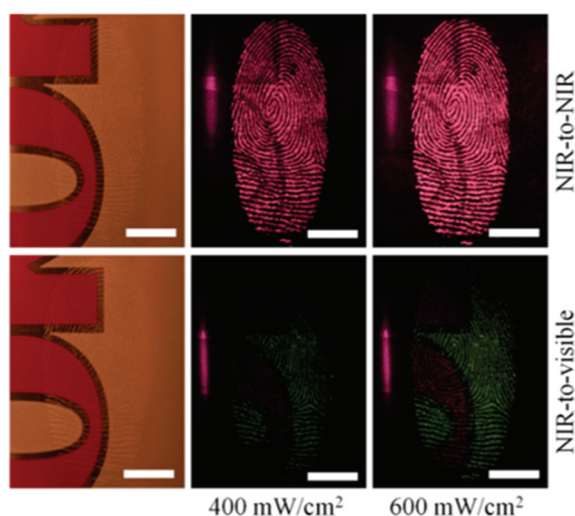
conditions and consequently difficult to duplicate or fake in contrast to organic dyes⁵⁵. A QR code can hold more data than the traditional barcode but is not suitable for security applications. For anti-counterfeiting applications, invisible QR codes can be printed using UCL ink that can be protected by coating with an opaque protective layer without adversely affecting functionality⁵⁶. Hiding NIR luminescent letters or symbols in a color print enhances the security level of color prints. UCL ink can be printed onto various surfaces such as paper or plastic substrates. Prints of letters “UCNP” and a football are hidden into a non-luminescent color print of a butterfly, enhancing the anti-counterfeiting strength⁵⁷.

Latent Fingerprinting

Finger marks are considered as one of the most valuable types of physical evidence for effective identification at crime scenes. Conventional latent fingerprinting methods that have been achieved using metallic, magnetic or fluorescent powders are ineffective

Table 1. Upconversion nanomaterial-based detection tools for numerous analytes.

Upconversion nanomaterial	Emission (980 nm excitation)	Analyte	Dynamic range (LOD)	Assay format	Ref.
NaYF ₄ :Yb,Tm@NaYF ₄ :Ca	800, 650, 450 nm	Avian Influenza Virus	H5N6 / H5N2 (10 ² / 10 ^{3.5} EID ₅₀ /mL)	Lateral Flow Immunoassay	32
NaYF ₄ :Yb,Er	660, 550, 530 nm	Alpha-Fetoprotein	0.01 – 40 ng/mL (5.3 pg/mL)	Microplate Immunoassay	33
NaYF ₄ :Yb,Er	656, 540 nm	Diclofenac	0 – 10 ng/mL (0.05 ng/mL)	ELISA	34
NaYF ₄ :Yb,Er@NaLuF ₄	546 nm	Myoglobin	0.5 – 400 ng/mL	Lateral Flow Assay	28
NaYF ₄ :Yb,Er/Tm	800, 450 nm	Prostate-Specific Antigen	0.1 – 100 pg/mL (23.0 fg/mL)	ELISA	31
NaYF ₄ :Yb,Er@NaGdF ₄	655, 541 nm	Caspase-9 Activity	0.5 – 100 U/mL (0.068 U/mL)	LRET-based	36
NaYF ₄ :Yb,Er@NaYF ₄	585 nm	Exosomes	(80 particles/μL)	LRET-based Aptasensor	37
NaYF ₄ @NaYF ₄ :Yb,Tm@NaYF ₄	800 nm	Progesterone	30 – 1000 pg/mL (1.36 pg/mL)	LRET-based Immunoassay	38
NaYF ₄ :Yb,Er	554 nm	Pb ²⁺ Ions	0.5– 10 μM (20 nM)	LRET-based	39
LiYF ₄ :Yb,Er,Ho,Tm@LiYF ₄ :Yb	650nm, 540nm, 475nm	Hg ²⁺ Ions	0 – 80 mM	LRET-based	40
NaYF ₄ :Yb,Er	660, 550 nm	pH	pH 2.5 – 7.2	LRET-based	41
NaGdF ₄ :Yb,Er	650 nm	pH	pH 6 – 8	LRET-based	42

**Figure 7.** Latent fingerprints developed with NIR-to-NIR (top row) and NIR-to-visible (bottom row) UCNP⁶⁰. Images reproduced from the references with permission.

on certain substrates like wet objects. To improve contrast, sensitivity, and selectivity, UCL-based latent fingerprinting was developed using NIR-to-visible UCNPs (NaYF₄:Yb,Er)⁵⁸. Fingerprints on a variety of substrates can be performed without necessitating a background signal noise interference and the minute features, including sweat pores can be observed clearly; this is because of NIR excitation and nanosized UCNPs. In addition, latent fingermarks aged for up to 1 year can be developed with clear ridges⁵⁹. For effective fingerprint imaging in full room light, NIR-to-NIR UCNP can be used, which is significantly brighter than NIR-to-visible UCNP (Figure 7). Images obtained at 800 nm suffer less from the background signal noise interference on substrates; this is because numerous inks cannot absorb at the 800 nm emission wavelength of NIR-to-NIR UCNP⁶⁰.

Conclusions and Future Perspective

Over the past decades, a variety of studies has been

identified not only efficient synthetic approaches that have enabled the synthesis of high quality UCNPs but also upconversion optical properties such as a large anti-Stokes shift, narrow emission spectra and long excited-state lifetime. In this review, we highlighted the overview of UCNPs and their recent applications. Contrast to the traditional fluorescent materials (e.g., organic dyes and quantum dots), the UCNPs overcome the traditional challenges such as photo-bleaching, surface modification and toxicity. Consequently, due to the unique optical properties of UCNPs (especially less autofluorescence and deeper penetration upon NIR irradiation), UCL-based platforms have turned out to be a promising tool for detecting analytes, bioimaging, and therapies. In particular, the NIR-to-NIR signal based detection system called the diagnostic window (650 ~ 800 nm) was able to detect signals in opaque samples and serum-based samples. Furthermore, the utilization of NIR has broadened their applications in energy harvesting and conversion as well as security printing. However, despite the great potential of UCNPs, several challenges exist that must be addressed. 1) The relatively low quantum yield of UCNPs attributes to their low extinction coefficient (an intrinsic feature of $4f$ optical transitions in lanthanide dopant ions). Therefore, UCNPs only play a secondary role in the solar energy conversion. 2) The UCNPs are generally excited under 980 nm irradiation owing to the overlapping with the absorption of sensitizer Yb^{3+} ions. However, it well-matched with the absorption of water, which could cause the overheating effect in biological environments. In the future, systematic studies to overcome these limitations of UCNPs can be a great stimulus for the next generation of luminescence-based applications.

Acknowledgements This study was partly supported by a grant from the Korea Institute of Science and Technology Institutional Program (2E26990/CAP-16-02-KIST) and the Bio & Medical Technology Development Programs (NRF-2016M3A9B6902060) through the Ministry of Science, ICT & Future Planning.

Conflict of Interests The authors declare no competing financial interests.

References

- Shen, J., Sun, L.D. & Yan, C.H. Luminescent rare earth nanomaterials for bioprobe applications. *Dalton Trans.* 5687-5697 (2008).
- Bae, P.K., So, H.-M., Kim, K. N., You, H.S., Choi, K.S., Kim, C.H., Park, J.-K. & Lee, J.-O. Simple route for the detection of Escherichia coli using quantum dots. *BioChip J.* **4**, 129-133 (2010).
- Pinaud, F., Michalet, X., Bentolila, L.A., Tsay, J.M., Doose, S., Li, J.J., Iyer, G. & Weiss, S. Advances in fluorescence imaging with quantum dot bio-probes. *Biomaterials* **27**, 1679-1687 (2006).
- Kim, M.J., Zheng, S., Kim, T.S. & Kim, S.K. Analysis of DNA coverage using enzymatic cleavage of fluorescent labels. *BioChip J.* **5**, 39-46 (2011).
- Yang, L.-H., Ahn, D.J. & Koo, E. An ultrasensitive FRET-based DNA sensor via the accumulated QD system derivatized in the nano-beads. *BioChip J.* **12**, 340-347 (2018).
- Kobayashi, H., Ogawa, M., Alford, R., Choyke, P.L. & Urano, Y. New strategies for fluorescent probe design in medical diagnostic imaging. *Chem. Rev.* **110**, 2620-2640 (2010).
- Algar, W.R., Kim, H., Medintz, I.L. & Hildebrandt, N. Emerging non-traditional Förster resonance energy transfer configurations with semiconductor quantum dots: Investigations and applications. *Coord. Chem. Rev.* **263-264**, 65-85 (2014).
- Zhang, Z., Shikha, S., Liu, J., Zhang, J., Mei, Q. & Zhang, Y. Upconversion nanoprobe: Recent advances in sensing applications. *Anal. Chem.* **91**, 548-568 (2019).
- Zhou, B., Shi, B., Jin, D. & Liu, X. Controlling upconversion nanocrystals for emerging applications. *Nat. Nanotechnol.* **10**, 924-936 (2015).
- Chen, G., Qiu, H., Prasad, P.N. & Chen, X. Upconversion nanoparticles: design, nanochemistry, and applications in theranostics. *Chem. Rev.* **114**, 5161-5214 (2014).
- Auzel, F. Upconversion processes in coupled ion systems. *J. Lumin.* **45**, 341-345 (1990).
- Bloembergen, N. Solid State Infrared Quantum Counters. *Phys. Rev. Lett.* **2**, 84-85 (1959).
- Auzel, F. Upconversion and anti-stokes processes with f and d ions in solids. *Chem. Rev.* **104**, 139-174 (2004).
- Cavalli, E., Angiuli, F., Belletti, A. & Boutinaud, P. Luminescence spectroscopy of $\text{YVO}_4:\text{Ln}^{3+}, \text{Bi}^{3+}$ ($\text{Ln}^{3+}=\text{Eu}^{3+}, \text{Sm}^{3+}, \text{Dy}^{3+}$) phosphors. *Opt. Mater.* **36**, 1642-1648 (2014).
- Heer, S., Kömpe, K., Güdel, H.-U. & Haase, M. Highly efficient multicolour upconversion emission in transparent colloids of lanthanide-doped NaYF_4 nanocrystals. *Adv. Mater.* **16**, 2102-2105 (2004).
- Shan, J., Kong, W., Wei, R., Yao, N. & Ju, Y. An investigation of the thermal sensitivity and stability of the $\beta\text{-NaYF}_4:\text{Yb}, \text{Er}$ upconversion nanophosphors. *J. Appl. Phys.* **107**, 054901 (2010).

17. Singh, B.P., Parchur, A.K., Singh, R.K., Ansari, A.A., Singh, P. & Rai, S.B. Structural and up-conversion properties of Er³⁺ and Yb³⁺ co-doped Y₂Ti₂O₇ phosphors. *Phys. Chem. Chem. Phys.* **15**, 3480-3489 (2013).
18. Payrer, E.L., Joudrier, A.L., Aschehoug, P., Almeida, R.M. & Deschanvres, J.L. Up-conversion luminescence in Er/Yb-doped YF₃ thin films deposited by PLI-MOCVD. *J. Lumin.* **187**, 247-254 (2017).
19. Arppe, R., Hyppänen, I., Perälä, N., Peltomaa, R., Kaiser, M., Würth, C., Christ, S., Resch-Genger, U., Schäferling, M. & Soukka, T. Quenching of the up-conversion luminescence of NaYF₄:Yb³⁺,Er³⁺ and NaYF₄:Yb³⁺,Tm³⁺ nanophosphors by water: the role of the sensitizer Yb³⁺ in non-radiative relaxation. *Nanoscale* **7**, 11746-11757 (2015).
20. Liu, J., Huang, L., Tian, X., Chen, X., Shao, Y., Xie, F., Chen, D. & Li, L. Magnetic and fluorescent Gd₂O₃:Yb³⁺/Ln³⁺ nanoparticles for simultaneous upconversion luminescence/MR dual modal imaging and NIR-induced photodynamic therapy. *Int. J. Nanomed.* **12**, 1-14 (2016).
21. Shen, J., Chen, G., Ohulchanskyy, T. Y., Kesseli, S. J., Buchholz, S., Li, Z., Prasad, P. N. & Han, G. Tunable near infrared to ultraviolet upconversion luminescence enhancement in (alpha-NaYF₄:Yb, Tm)/CaF₂ core/shell nanoparticles for in situ real-time recorded biocompatible photoactivation. *Small* **9**, 3213-3217 (2013).
22. Wisser, M. D., Fischer, S., Siefe, C., Alivisatos, A. P., Salleo, A. & Dionne, J. A. Improving quantum yield of upconverting nanoparticles in aqueous media via emission sensitization. *Nano Lett.* **18**, 2689-2695 (2018).
23. Wilhelm, S. Perspectives for upconverting nanoparticles. *ACS Nano* **11**, 10644-10653 (2017).
24. Zhang, Y.-W., Sun, X., Si, R., You, L.-P. & Yan, C.-H. Single-crystalline and monodisperse LaF₃ Triangular Nanoplates from a single-source precursor. *J. Am. Chem. Soc.* **127**, 3260-3261 (2005).
25. Mai, H.-X., Zhang, Y.-W., Si, R., Yan, Z.-G., Sun, L.-d., You, L.-P. & Yan, C.-H. High-quality sodium rare-earth fluoride nanocrystals: Controlled synthesis and optical properties. *J. Am. Chem. Soc.* **128**, 6426-6436 (2006).
26. Shan, J., Qin, X., Yao, N. & Ju, Y. Synthesis of monodisperse hexagonal NaYF₄:Yb, Ln (Ln = Er, Ho and Tm) upconversion nanocrystals in TOPO. *Nanotechnology* **18**, 445607 (2007).
27. Yi, G., Lu, H., Zhao, S., Ge, Y., Yang, W., Chen, D. & Guo, L.-H. Synthesis, characterization, and biological application of size-controlled nanocrystalline NaYF₄:Yb,Er infrared-to-visible up-conversion phosphors. *Nano Lett.* **4**, 2191-2196 (2004).
28. Ji, T., Xu, X., Wang, X., Zhou, Q., Ding, W., Chen, B., Guo, X., Hao, Y. & Chen, G. Point of care up-conversion nanoparticles-based lateral flow assay quantifying myoglobin in clinical human blood samples. *Sens. Actuators, B* **282**, 309-316 (2019).
29. Farka, Z., Mickert, M.J., Hlaváček, A., Skládal, P. & Gorris, H.H. Single molecule upconversion-linked immunosorbent assay with extended dynamic range for the sensitive detection of diagnostic biomarkers. *Anal. Chem.* **89**, 11825-11830 (2017).
30. Gong, Y., Zheng, Y., Jin, B., You, M., Wang, J., Li, X., Lin, M., Xu, F. & Li, F. A portable and universal upconversion nanoparticle-based lateral flow assay platform for point-of-care testing. *Talanta* **201**, 126-133 (2019).
31. Mickert, M. J., Farka, Z., Kostiv, U., Hlaváček, A., Horák, D., Skládal, P. & Gorris, H.H. Measurement of sub-femtomolar concentrations of prostate-specific antigen through single-molecule counting with an upconversion-linked immunosorbent assay. *Anal. Chem.* **91**, 9435-9441 (2019).
32. Kim, J., Kwon, J.H., Jang, J., Lee, H., Kim, S., Hahn, Y.K., Kim, S.K., Lee, K.H., Lee, S., Pyo, H., Song, C.S. & Lee, J. Rapid and background-free detection of avian influenza virus in opaque sample using NIR-to-NIR upconversion nanoparticle-based lateral flow immunoassay platform. *Biosens. Bioelectron.* **112**, 209-215 (2018).
33. Luo, Z., Zhang, L., Zeng, R., Su, L. & Tang, D. Near-infrared light-excited core-core-shell UCNP @Au@CdS upconversion nanospheres for ultrasensitive photoelectrochemical enzyme immunoassay. *Anal. Chem.* **90**, 9568-9575 (2018).
34. Hlaváček, A., Farka, Z., Hübner, M., Horňáková, V., Němeček, D., Niessner, R., Skládal, P., Knopp, D. & Gorris, H.H. Competitive upconversion-linked immunosorbent assay for the sensitive detection of diclofenac. *Anal. Chem.* **88**, 6011-6017 (2016).
35. Takkinen, K. & Zvirbliene, A. Recent advances in homogenous immunoassays based on resonance energy transfer. *Curr. Opin. Biotechnol.* **55**, 16-22 (2019).
36. Liu, L., Zhang, H., Wang, Z. & Song, D. Peptide-functionalized upconversion nanoparticles-based FRET sensing platform for Caspase-9 activity detection in vitro and in vivo. *Biosens. Bioelectron.* **141**, 111403 (2019).
37. Wang, Y., Luo, D., Fang, Y., Wu, W., Wang, Y., Xia, Y., Wu, F., Li, C., Lan, J. & Chen, J. An aptasensor based on upconversion nanoparticles as LRET donors for the detection of exosomes. *Sens. Actuators B Chem.* **298**, 126900 (2019).
38. Kang, D., Lee, S., Shin, H., Pyun, J. & Lee, J. An efficient NIR-to-NIR signal-based LRET system for homogeneous competitive immunoassay. *Biosens. Bioelectron.* **150**, 111921 (2020).
39. Zhang, Y., Wu, L., Tang, Y., Su, Y. & Lv, Y. An up-

- conversion fluorescence based turn-on probe for detecting lead(ii) ions. *Anal. Methods*. **6**, 9073-9077 (2014).
40. Liu, Q., Peng, J., Sun, L. & Li, F. High-efficiency up-conversion luminescent sensing and bioimaging of Hg(II) by chromophoric ruthenium complex-assembled nanophosphors. *ACS Nano* **5**, 8040-8048 (2011).
 41. Arppe, R., Näreoja, T., Nylund, S., Mattsson, L., Koho, S., Rosenholm, J. M., Soukka, T. & Schäferling, M. Photon upconversion sensitized nanoprobe for sensing and imaging of pH. *Nanoscale* **6**, 6837-6843 (2014).
 42. Wang, S., Feng, J., Song, S. & Zhang, H. A long-wave optical pH sensor based on red upconversion luminescence of NaGdF₄ nanotubes. *RSC Adv.* **4**, 55897-55899 (2014).
 43. Li, Y., Gu, Y., Yuan, W., Cao, T., Li, K., Yang, S., Zhou, Z. & Li, F. Core-shell-shell NaYbF₄:Tm@CaF₂@NaDyF₄ Nanocomposites for Upconversion/T2-Weighted MRI/Computed Tomography Lymphatic Imaging. *ACS Appl. Mater. Interfaces* **8**, 19208-19216 (2016).
 44. Lee, J., Gordon, A. C., Kim, H., Park, W., Cho, S., Lee, B., Larson, A.C., Rozhkova, E.A. & Kim, D.H. Targeted multimodal nano-reporters for pre-procedural MRI and intra-operative image-guidance. *Biomaterials* **109**, 69-77 (2016).
 45. Xu, J., Yang, P., Sun, M., Bi, H., Liu, B., Yang, D., Gai, S., He, F. & Lin, J. Highly emissive dye-sensitized up-conversion nanostructure for dual-photosensitizer photodynamic therapy and bioimaging. *ACS Nano* **11**, 4133-4144 (2017).
 46. Sun, M., Xu, L., Ma, W., Wu, X., Kuang, H., Wang, L. & Xu, C. Hierarchical plasmonic nanorods and upconversion core-satellite nanoassemblies for multimodal imaging-guided combination phototherapy. *Adv. Mater.* **28**, 898-904 (2016).
 47. Xu, J., Han, W., Yang, P., Jia, T., Dong, S., Bi, H., Gulzar, A., Yang, D., Gai, S., He, F., Lin, J. & Li, C. Tumor microenvironment-responsive mesoporous MnO₂-coated upconversion nanoplatform for self-enhanced tumor theranostics. *Adv. Funct. Mater.* **28** (2018).
 48. Kuk, S., Lee, B.I., Lee, J.S. & Park, C.B. Rattle-structured upconversion nanoparticles for near-IR-induced suppression of Alzheimer's beta-amyloid aggregation. *Small* **13** (2017).
 49. Fan, W., Bu, W. & Shi, J. On the latest three-stage development of nanomedicines based on upconversion nanoparticles. *Adv. Mater.* **28**, 3987-4011 (2016).
 50. Frederick, J.E., Snell, H.E. & Haywood, E.K. Solar ultraviolet radiation at the earth's surface. *Photochem. Photobiol.* **50**, 443-450 (1989).
 51. Lee, S.H., Kim, J.H. & Park, C.B. Coupling photocatalysis and redox biocatalysis toward biocatalyzed artificial photosynthesis. *Chem. - Eur. J.* **19**, 4392-4406 (2013).
 52. Kim, H., You, Y., Kang, D., Jeon, D., Bae, S., Shin, Y., Lee, J., Lee, J. & Ryu, J. Modular layer-by-layer assembly of polyelectrolytes, nanoparticles, and molecular catalysts into solar-to-chemical energy conversion devices. *Adv. Funct. Mater.* **29**, 1906407 (2019).
 53. Lee, J.S., Lee, S.H., Kim, J. & Park, C.B. Graphene-Rh-complex hydrogels for boosting redox biocatalysis. *J. Mater. Chem. A* **1**, 1040-1044 (2013).
 54. Lee, J.S., Nam, D.H., Kuk, S.K. & Park, C.B. Near-infrared-light-driven artificial photosynthesis by nanobiocatalytic assemblies. *Chem. - Eur. J.* **20**, 3584-3588 (2014).
 55. Yao, W., Tian, Q., Liu, J., Wu, Z., Cui, S., Ding, J., Dai, Z. & Wu, W. Large-scale synthesis and screen printing of upconversion hexagonal-phase NaYF₄:Yb³⁺,Tm³⁺/Er³⁺/Eu³⁺ plates for security applications. *J. Mater. Chem. C* **4**, 6327-6335 (2016).
 56. Baride, A., Meruga, J.M., Douma, C., Langerman, D., Crawford, G., Kellar, J.J., Cross, W.M. & May, P.S. A NIR-to-NIR upconversion luminescence system for security printing applications. *RSC Adv.* **5**, 101338-101346 (2015).
 57. Liu, H., Xu, J., Wang, H., Liu, Y., Ruan, Q., Wu, Y., Liu, X. & Yang, J.K.W. Tunable resonator-upconverted emission (TRUE) color printing and applications in optical security. *Adv. Mater.* **31**, 1807900 (2019).
 58. Wang, M. Latent fingerprints light up: facile development of latent fingerprints using NIR-responsive upconversion fluorescent nanocrystals. *RSC Adv.* **6**, 36264-36268 (2016).
 59. Wang, M., Li, M., Yang, M., Zhang, X., Yu, A., Zhu, Y., Qiu, P. & Mao, C. NIR-induced highly sensitive detection of latent fingerprints by NaYF₄:Yb,Er upconversion nanoparticles in a dry powder state. *Nano Res.* **8**, 1800-1810 (2015).
 60. Baride, A., Sigdel, G., Cross, W.M., Kellar, J.J. & May, P.S. Near infrared-to-near infrared upconversion nanocrystals for latent fingerprint development. *ACS Appl. Nano Mater.* **2**, 4518-4527 (2019).